Hydrogen-Bonding Strength in the Blends of Polybenzimidazole with BTDA- and DSDA-Based Polyimides

Tae-Kwang Ahn, Mojun Kim, and Soonja Choe*

Department of Chemical Engineering, Institute of Polymer Science and Engineering, Inha University, Inchon 402-751, Republic of Korea

Received November 27, 1995; Revised Manuscript Received August 27, 1996[⊗]

ABSTRACT: Blends of solutions of poly[2,2′-(*m*-phenylene)-5,5′-bibenzimidazole] (PBI) with poly(amic acids) (PAA's) synthesized from BTDA (3,3′,4,4′-tetracarboxybenzophenone dianhydride) and DSDA (3,3′,4,4′-tetracarboxydiphenyl sulfone dianhydride) with 3,3′-DDSO$_2$ (3,3′-diaminodiphenyl sulfone), 4,4′-DDSO$_2$ (4,4′-diaminodiphenyl sulfone), 4,4′-MDA (4,4′-methylenedianiline), and 4,4′-ODA (4,4′-oxydianiline) were prepared in DMAc solvent and transformed into PBI/polyimide (PI) blends by curing at higher temperatures than the T_gs of the blends. The blend systems used in this study were all miscible; evidences for miscibility were optically clear film, a synergistic single T_gs at all compositions, and frequency shifts of the functional groups intermediate between those of the constituents. The strength of intermolecular interaction between PBI and various polyimides were measured by means of DSC, DMTA, and FT-IR. From the analyzed data based on the T_g diagram, the Fox equation, the k values in Gordon−Taylor equation, and the frequency shifts of the functional groups, interpretation was consistent, implying that the strengths of hydrogen bonding display relatively higher in the BTDA-based blends than the DSDA systems. This difference may be arised from the electron affinity in the spacer between benzophenone carbonyl in BTDA and symmetric sulfone in DSDA.

Introduction

Because of superior thermal stability, thermooxidative stability, mechanical properties, and chemical resistances, polyimides (PI) prepared from various aromatic dianhydrides and diamines have been used in the form of films, pellets, sheets, or solutions.[1] This material has been used as a new material, substituting for glasses or metals in various fields of the electrical, electronics, coatings, high temperature adhesives, or aerospace industries.[2] In particular, for the purpose of specific applications, characterization studies of polyimides consisting of various structures have been carried out systematically.[2−7] Aromatic polybenzimidazole (PBI) has been applied to fire clothing, clothing for spacecraft crewmen, or industries requiring thermal and chemical stability due to its high thermal stability (T_g 420 °C), inflammability, or outstanding mechanical properties.[8] This material is expected to find new uses in for high temperature adhesives, ion exchange resins, batteries, foams, and microporous absorbent beads and so on.

Studies of the blends in aromatic PBI with various commercial polyimides such as Ultem 1000 of General Electric, XU 218 of Ciba-Geigy, PI 2080 of Dow Chemical, or LaRC TPI of Mitsui Toatsu have been carried out to investigate the miscibility dependent upon the structures of polyimides, the phase behavior, or specific interactions for miscibility over the past several years.[9−14] Finding miscibility in PBI/PI blend systems was not always the case. An immiscible blend[15] was discovered from an opaque cast film and two T_gs, each of which was characteristic of the constituents, whereas miscible systems were observed in the form of transparent films, with single composition dependent T_gs intermediate of those for the component polymers and band shift phenomena reflecting the functional groups in FT-IR spectroscopy studies. Blend systems of PBI and various polyimide structures which possess nearly nonpolar spacers between phenyl rings showed miscibility, and

hydrogen bonding between the N−H group of PBI and the C=O group of PI was reported to be the most important factor inducing miscibility.[10,13−18] However, as a method for choosing the blend system between PBI and PIs, there is a structural limitation due to PI because of the poor solubility of polyimides. To compensate for the shortcomings due to the poor solubility of fully imidized polyimides, PBI/PI blends cured from PBI/poly(amic acid) (PAA) are suggested to be one of the ways to solve the above limitation.[12,16]

In this study, blends of PBI with poly(amic acids)[16] synthesized from two dianhydrides, BTDA and DSDA, and four diamines, 3,3′-DDSO$_2$, 4,4′-DDSO$_2$, 4,4′-MDA, and 4,4′-ODA, were at first prepared by solution mixing of two polymers and were fully imidized by curing the PBI/PAA solutions as if they were a kind of PBI/PI system. Miscibility was investigated in term of the single T_gs for all of the blend compositions and also the frequency shifts of the functional groups. In addition, the area between the measured T_g and the Fox equation or the k values in the Gordon−Taylor equation[19] was used to compare the strength of the intermolecular interaction, which is rationalized as hydrogen bonding. Then the relative difference in the strengths of hydrogen bonding between the BTDA and the DSDA blend systems was rationalized.

Experimental Section

Synthesis of Poly(amic acid) and Blend Preparation. BTDA and DSDA as dianhydrides and 3,3′-DDSO$_2$, 4,4′-DDSO$_2$, 4,4′-ODA were purchased from Chriskev Co., Kansas City, MO, and 4,4′-MDA was obtained from Hodogaya Co., Japan. Since dianhydrides tend to acidify to carboxylic acid by absorbing moisture in air, they were dried in vacuum oven at higher than the melting temperature of the monomer for 30 min and then immediately used for synthesis. PBI was obtained from Celanese Fiber Corp. (Lot. No. 90330; T_g = 424 °C) and then used as received (powder) after drying at 300 °C for 1 h. The chemical structures and information are listed in Figure 1. The solvent DMAc (*N,N*-dimethylacetamide; bp = 165−166 °C) was purchased from Aldrich Chemical Co. and used as received.
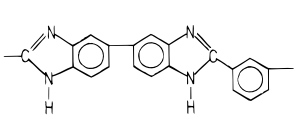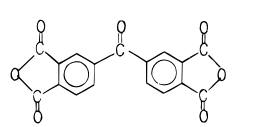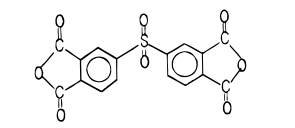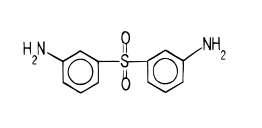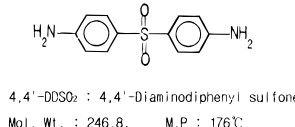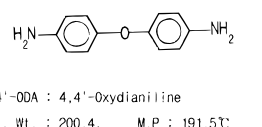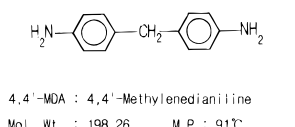
PAA in a 15 wt % solution in DMAc was synthesized with a precise stoichiometric ratio between dianhydrides and di-

Table 1. Characterization Data of PBI/PI Blend Systems

blend system	T_g of the PI (°C)	area[a]	k	C=O (1724 cm^{-1} [b]/ 1731 cm^{-1} [c])	C=O (1780 cm^{-1})	N—H (3418 cm^{-1})
				band shift		
PBI/BTDA + 3,3′–DDSO$_2$ (BTDA I)	273	118	1.02	9	4	53
PBI/DSDA + 3,3′–DDSO$_2$ (DSDA I)	255	12	0.83	5	3	41
PBI/BTDA + 4,4′–DDSO$_2$ (BTDA II)	329	115	1.41	9	4	52
PBI/DSDA + 3,3′–DDSO2 (DSDA II)	310	0	1.36	5	3	40
PBI/BTDA + 4,4′–MDA (BTDA III)	293	182	1.74	7	3	50
PBI/DSDA + 4,4′–MDA (DSDA III)	282	64	1.12	5	3	40
PBI/BTDA + 4,4′–ODA (BTDA IV)	294	190	2.13	7	3	53
PBI/DSDA + 4,4′–ODA (DSDA IV)	287	88	0.93	6	4	39

[a] Area was calculated by the difference between the experimental T_gs and the calculated T_gs by the Fox equation. [b] BTDA systems. [c] DSDA systems.

Figure 1. Chemical structures and characteristics of monomers.

amines by stirring for 24 h and precipitated into a powder in distilled water to remove the remaining unreacted monomers or impurities in the PAA solution followed by drying at 80 °C for several hours. Then the PAA powder was again dissolved in a 3 wt % solution using DMAc. PBI was dissolved in DMAc at 225 °C and 40 psi for 30 min in a high-pressure vessel (Parr Instrument Co.), and prepared in a 3 wt % solution after filtering undissolved residues of about 0.3 wt %. Since the fully imidized polyimides synthesized in this study mostly show poor solubility, PBI and eight different PAA solutions were mixed in various weight ratios by stirring for 3 h. The PBI/PAA blends were precipitated into distilled water or cast as a film on a glass plate and then cured at 30 °C higher than the estimated T_g of each PI using the Fox equation.

PBI/BTDA + 3,3′-DDSO$_2$, PBI/BTDA + 4,4′-DDSO$_2$, PBI/BTDA + 4,4′-MDA, and PBI/BTDA + 4,4′-ODA were named as the BTDA I, BTDA II, BTDA III, and BTDA IV systems, respectively, for convenience, and the DSDA systems with PBI/DSDA + 3,3′-DDSO$_2$, PBI/DSDA + 4,4′-DDSO$_2$, PBI/DSDA + 4,4′-MDA, and PBI/DSDA + 4,4′-ODA named as the blends

DSDA I, DSDA II, DSDA III, and DSDA IV, respectively, and they are listed in Table 1. The cast film for FT-IR spectroscopy study was thin enough to obey the absorbance range of the Beer–Lambert law.[13] Blend samples were kept in a desiccator before analysis in order to inhibit moisture absorption.

Instrumentation. Powder samples of 5–20 mg were scanned from 50 °C to the desired temperature at a heating rate of 20 °C/min using a Perkin-Elmer DSC-7, annealed at that temperature for 10 min, quenched to room temperature at 200 °C/min, and rescanned to the desired temperature at the same heating rate. The data were collected from the second scan, and the averages of five different measurements were used for investigation of the T_gs and miscibility.

A Polymer Laboratories DMTA Mk III was used to measure the T_gs at a scanning rate of 4 °C/min from 50 °C to the desired temperature under tensile mode, strain of 1%, and 5 Hz using a specimen with appropriate size for measurement.

FT-IR studies were performed using a Bruker FTS-48 spectroscope at a resolution of 2 cm^{-1} and signals of the average of 30 scans with 1–5 μm thick film.

Analysis. For each blend system, the single composition dependent T_gs obtained by experiments and the T_gs calculated by using the Fox equation were used to calculate the area between two curves related two different T_gs to induce intermolecular interactions. The best fit k value in the Gordon–Taylor equation was calculated by Prud'homme et al.[20] for each blend system.

Frequency shifts of the N–H and carbonyl stretching bands and band shapes were used to analyze the strength of the hydrogen bonding between BTDA and DSDA systems.

The areas obtained from the T_g and the k values were correlated to the frequency shifts of the functional groups in FTIR, and then the relative strengths of intermolecular interaction between the BTDA and DSDA systems are interpreted in terms of hydrogen bonding.

Results and Discussion

Thermal Properties of the Blends. To ensure the glass transition temperature (T_g) of the synthesized polyimides, powder or cast films which were fully cured from the poly(amic acids) were used. The second scan was used for the T_g collection of the system, and the T_gs were in good agreement with the previous reports and are listed in Table 1. These were used for calculation of the theoretical T_g of the blend with PBI by using the Fox equation or the k values in the Gordon–Taylor equation.

As a representative system, Figure 2 shows the DSC thermograms obtained from the second scan in BTDA I, where curves a and g are for homopolymers, PI and PBI, and curves b–f are for the 20, 30, 50, 70, and 80 wt % PBI in blends, respectively. The transparent film and single composition dependent T_gs were obtained for all of the blend compositions with the PBI component, showing that the system is miscible.
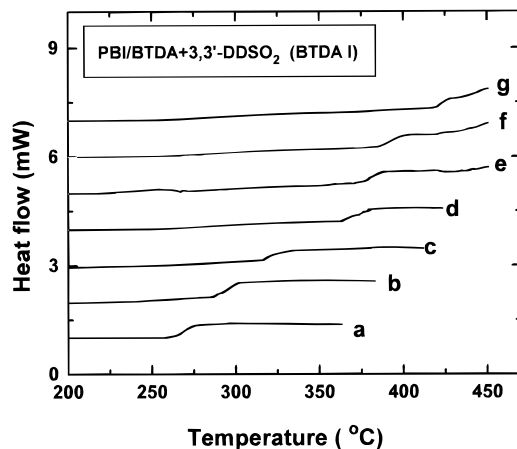
Figure 2. DSC thermograms of BTDA I obtained by the second scan: (a) pure PI; (b) PBI/PI = 20/80 wt %; (c) PBI/PI = 30/70 wt %; (d) PBI/PI = 50/50 wt %; (e) PBI/PI = 70/30 wt %; (f) PBI/PI = 80/20 wt %; (g) pure PBI.

In Figure 3a, the upper parabolic T_g diagram of the BTDA I system in the solid circles was obtained from the DSC measurement and compared with the calculated values from the Fox equation (dashed line). In particular, the 50/50 PBI/PI blend shows synergistic behavior compared to the other blend compositions, which suggests that this composition is strongly affected by intermolecular interactions between the two constituents.

The upper convex form of the T_g diagram was often regarded as being due to specific interactions[21-26] between two components, such as hydrogen bonding, donor–acceptor complex, etc. Examples are the blends of poly (styrene-*co*-vinylphenylbis(trifluoromethyl)carbinol) (PHFA)/bis(phenol A) polycarbonate and PHFA/poly(butyl methacrylate) systems[21] or Novolac A with atactic, isotactic, or syndiotactic PMMA and Novolac B with atactic, isotactic, or syndiotactic PMMA systems.[22] In particular, Kwei calculated the parameter q from the composition dependent weight average value of the T_g and interpreted it as a contribution of specific interactions. He proposed that the higher value of q, the stronger are the intermolecular interactions that exist. The k value in the Gordon–Taylor equation or the q value in the Kwei equation is often used to represent the intermolecular interaction parameter. In the past, hydrogen bonding was suggested as one of the intermolecular interactions between the carbonyl of PI and the N–H groups of PBI in PBI/PI blends.[5,10,11,13,14]

The glass transition temperatures for the BTDA II were depicted as solid squares in Figure 3b. From the DSC experiment, BTDA II systems also show single T_g's which have values higher than those of the calculated ones for the whole range of blend compositions. The measured T_gs in the BTDA III are shown in Figure 3c (with solid triangles) and this is similar to the BTDA II system, where the T_gs are 20–30 °C higher than those of the expected ones. It was reported that the blend of PBI with LaRC TPI[12] (BTDA + DABP (3,3′-diaminobenzophenone)) did not show synergistic behavior, and the T_gs of the blends were nearly the same as the calculated ones by the Fox equation. The measurement of the T_g in BTDA IV was carried out using DMTA due to the hardly detectable T_g by DSC. On the basis of the DMTA thermograms observed by means of tan δ from the second scan, a T_g diagram was drawn in Figure 3d, where solid diamonds and the dashed line denote the measured T_gs and the calculated values, respec-
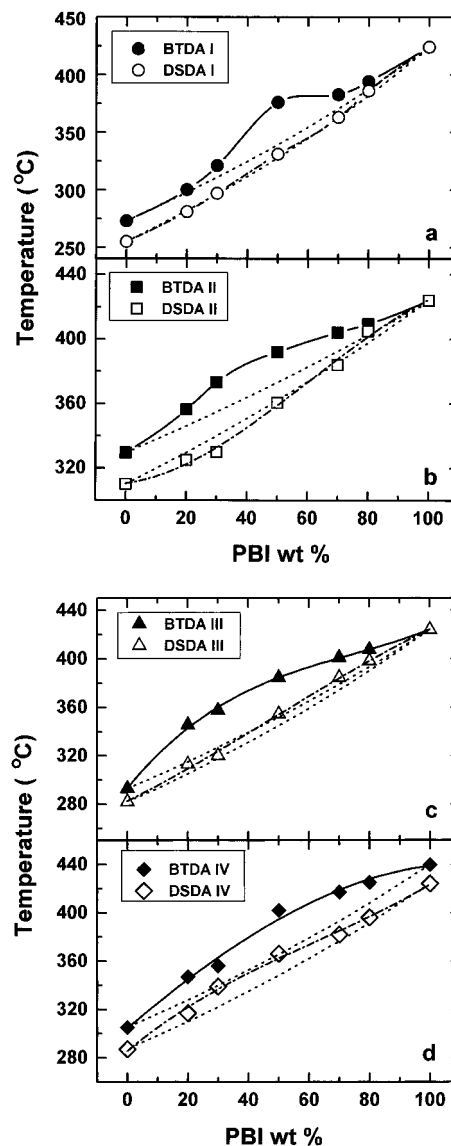
Figure 3. T_g diagram as a function of the blend compositions: (a) BTDA I (●), DSDA I (○); (b) BTDA II (■), DSDA II (□); (c) BTDA III (▲), DSDA III(△); (d) BTDA IV (◆), DSDA IV (◇) with T_gs by the Fox equation (- - -).

tively. This system also exhibits single composition dependent T_gs which are higher than the calculated ones.

The T_g diagrams obtained by DSC for the DSDA, I, II, III, and IV systems were also displayed in parts a–d of Figure 3, respectively, with the same open symbols with the BTDAs using solid symbols for comparison. Again the theoretical T_gs by the Fox equation were also plotted as dashed lines. Interesting features were observed between BTDA and DSDA systems as follows. In parts a and b of Figure 3, the experimental T_gs of the DSDA I and II systems are just on the lines of the calculated T_gs by the Fox equation, and this is the difference from the BTDA-based blends, which showed synergistic behavior. A similar trend was observed in the DSDA III and IV systems compared to the BTDA III and IV systems. For convenience, to compare the synergistic properties between the BTDA- and the DSDA-based systems, we calculated the area which was integrated between the experimental and the calculated T_g values of the Fox equation using computer regression, and they are listed as the area in Table 1. If this area is considered to represent the intensity of intermolecular

interactions, BTDA systems which display larger values of the area have stronger intermolecular interactions than the DSDA systems.

The analysis of intermolecular interaction was continued by interpreting the experimental results in terms of the Gordon–Taylor equation.[19] In this presentation, k represents $(\alpha_{r2} - \alpha_{g2})/(\alpha_{r1} - \alpha_{g1})$ (where α is the coefficient of thermal expansion, r and g represent the rubbery and glassy states, respectively, and 1 and 2 indicate the polymers 1 and 2), which indicates the magnitude of intermolecular interaction. In the absence of α data, k in the Gordon–Taylor equation, which shows the best fit with the experimental T_g, was determined by following Prud'homme et al.[20] The value of the Gordon–Taylor constant k can be related to the strength of interaction between the components in miscible polymer blends: the lower the value of k, the poorer is the interaction. The determination of the k value in the Gordon–Taylor equation is shown in Figure 4. These values are listed in Table 1. In a relatively recent work Masson and Manley found that T_gs of blends of cellulose and poly(4-vinylpyridine) (PVP) exhibit positive deviations from the mean value, while those of methyl cellulose and PVP exhibit negative deviations.[26] These results clearly indicate that strong specific interactions lead to positive deviations. In the cellulose–PVP system the strong interaction results from the hydrogen bonding between cellulose –OH and pyridine nitrogen in PVP. When the –OH group in cellulose is replaced by –OMe in methylcellulose, hydrogen bonding no longer occurs and the T_gs of the blends then exhibit negative deviation. In our miscible blend systems, as expected, k values become higher in the case of BTDA systems compared to DSDA systems, which can be rationalized to intermolecular specific interactions.

FT-IR Spectroscopic Studies of the Blends. The transformation of PBI/PAA into PBI/PI was confirmed by the T_g measurement from DSC or DMTA, or the band ratio of the 1720 cm^{-1} deformation of carbonyl to the internal standard[17] around 1520 cm^{-1}. In general, the carboxylic acid and the carbonyl stretching bands in PAA were observed near 3500 and 1720 cm^{-1}, respectively. Due to the imidization reaction, the hydroxyl band in carboxylic acid disappeared and a carbonyl band due to their heterocyclic 5-membered imide linkage simultaneously appeared near 1780 cm^{-1} including the 1724 cm^{-1} band. The above observation is used for verification of the PBI/PAA system being transformed into the PBI/PI system.

An investigation of the reason for miscibility was performed in terms of hydrogen bonding by analyzing the frequency shifts of the N–H and carbonyl bands as a function of the blend compositions. Then the degrees of the frequency shifts of the functional groups were used to differentiate the relative strengths of hydrogen bonding.
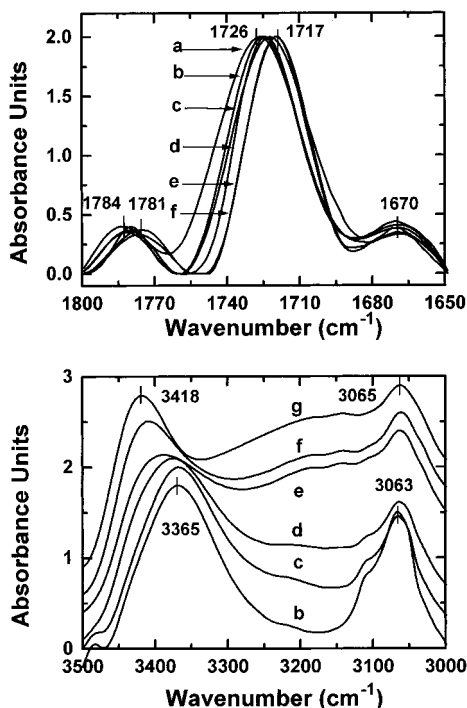
Representative carbonyl stretching bands of BTDA I are shown in Figure 5 (upper part) in the region of 1800–1650 cm^{-1}, where part a is the spectrum of pure PI and parts b–f are the spectra of 20, 30, 50, 70, and 80 wt % PBI content in the blends, respectively. For the BTDA-based polyimides, FT-IR spectra reveal three sorts of carbonyl bands, two of these arise from the carbonyl in the 5-membered imide ring and the third is from the benzophenone carbonyl group. The former is observed near 1780 and 1724 cm^{-1}, and the latter is observed near 1670 cm^{-1}. In the case of BTDA I as
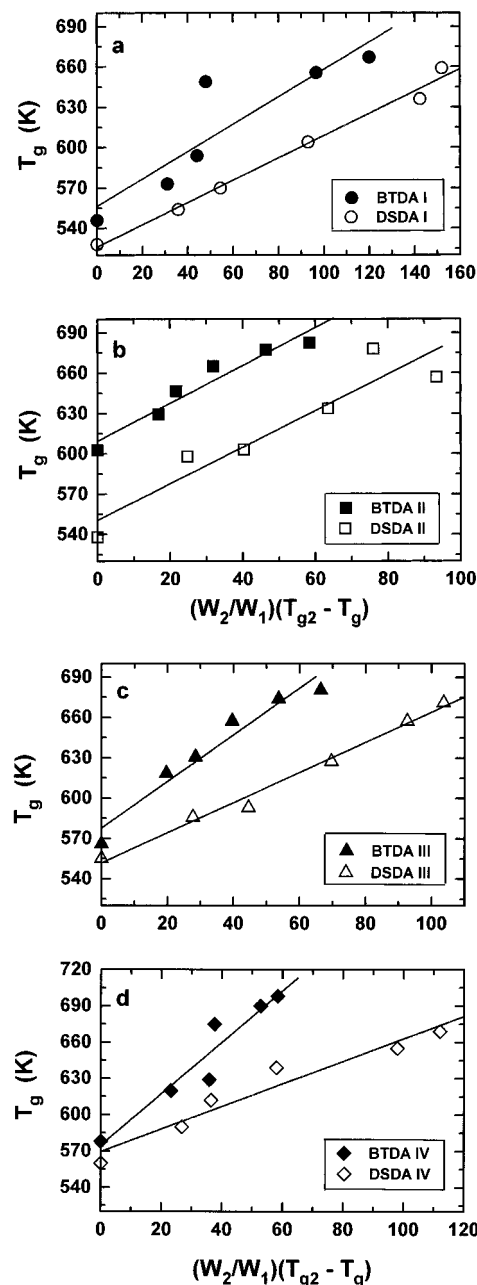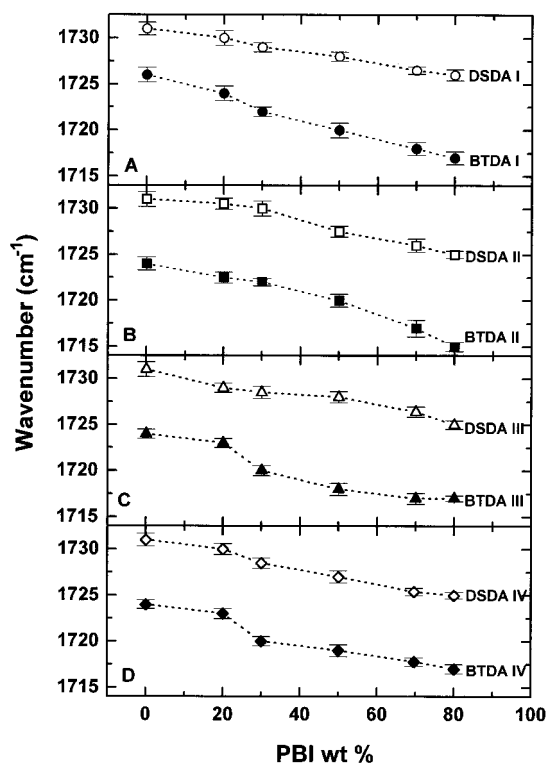

Figure 4. Plot of the Gordon–Taylor equation for blends where slope of the lines is equal to k: solid symbols, BTDA systems; open symbols, DSDA systems. The symbols are the same as in Figure 3.

shown in Figure 5 (upper spectra), the carbonyl band is observed at 1724 cm^{-1} in pure PI and linearly shifted to 1717 cm^{-1} at 80 wt % PBI in the blend. In addition, the carbonyl stretching near 1780 cm^{-1} was also lowered about 4 cm^{-1}. On the basis of these spectra, the aspects of the frequency shifts of the carbonyl band near 1726 cm^{-1} in the four blends systems including the BTDA I, II, III, and IV are presented in Figure 6 with the solid symbols (the same symbols used in the T_g diagram for convenience). The overall extent of these carbonyl band shifts is 9 cm^{-1} for BTDA I and II and 7 cm^{-1} for BTDA III and IV. In addition, the shapes of the frequency shifts are similar between BTDA I and II and between the BTDA III and IV.

The carbonyl band was expected to offer favorable conditions for hydrogen bonding with N–H group because of the presence of the lone pair of nitrogen in the 5-membered imide ring near 1780 cm^{-1}. Thus a
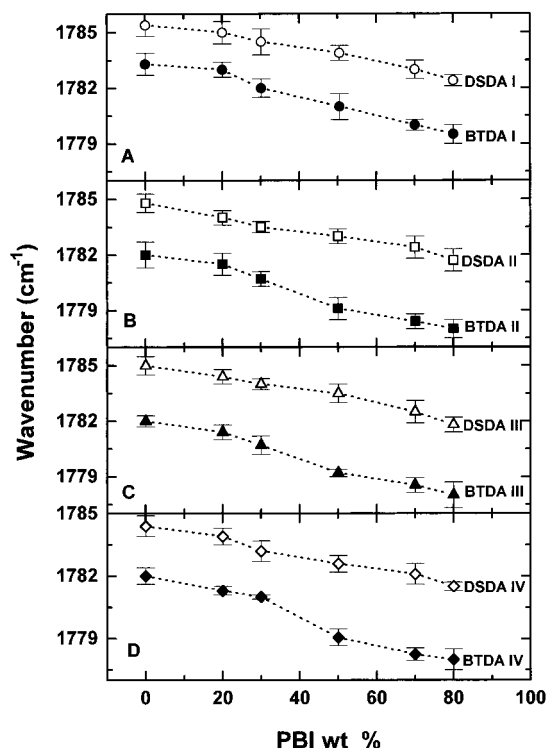
Figure 5. Representative FT-IR spectra in the 1800−1650 and 3500−3000 cm^{-1} regions in the BTDA I system: (a) pure PI; (b) 20 wt % PBI; (c) 30 wt % PBI; (d) 50 wt % PBI; (e) 70 wt % PBI; (f) 80 wt % PBI; (g) pure PBI.
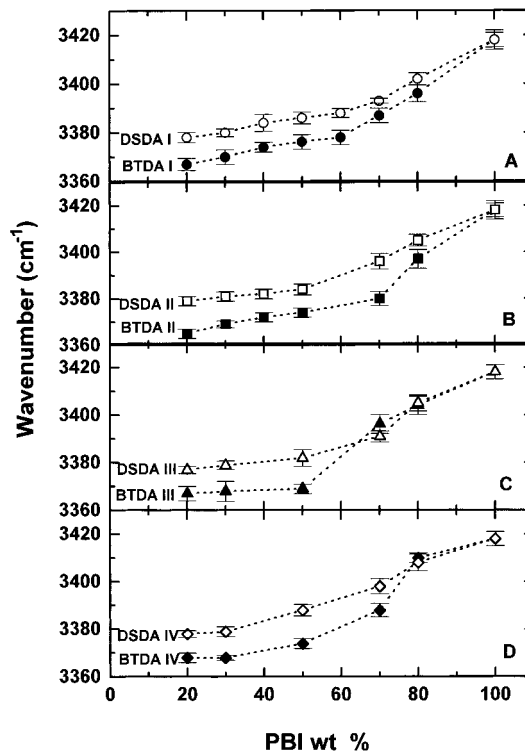

Figure 7. Frequency shifts of the carbonyl stretching near 1780 cm^{-1} as a function of PBI content.

Figure 6. Frequency shifts of the carbonyl stretching near 1724 or 1731 cm^{-1} in various blend systems.

Figure 8. Frequency shifts of the N−H stretching near 3418 cm^{-1} in various blend systems.

similar trend in frequency shifts near 1780 cm^{-1} was observed to be as much as 3−4 cm^{-1} for the four different BTDA systems and this was depicted in Figure 7 with the solid symbols for each system. On the other hand, no significant frequency shifts in the benzophenone carbonyl band near 1670 cm^{-1} was observed, indicating that the carbonyl between the two phenyl rings in BTDA does not participate in the formation of hydrogen bonding.

For discussion of the N−H group, FT-IR spectra of the region of 3500−3000 cm^{-1} for the BTDA I was also drawn in the lower part of Figure 5, where part g is the spectrum of pure PBI and parts b−f are the spectra of 20, 30, 50, 70, and 80 wt% PBI in the blends. The N−H stretching band is shifted to the lower frequency bound with PI content, while aromatic C−H band is constantly positioned at 3063 cm^{-1}. The extent of the band shifts shown in Figure 8 with the solid symbols are 53, 52,

50, and 53 cm^{-1} for the BTDA I, II, III, and IV systems, respectively.

From the above observation, the hydrogen bonding between the N–H group in PBI and the carbonyl stretching of the imide linkage was solely attributed to miscibility in PBI/BTDA systems. One more feature is that the N–H stretching band of PBI observed at 3418 cm^{-1} was dramatically shifted to a lower wavenumber by up to 50 wt % PI and then almost leveled off with a further incorporation of PI. This behavior suggests that the reaction of the functional groups by stoichiometric ratio attributes to a hydrogen bonding in the blends of PBI/PI.

In the PBI blends with DSDAs, spectral behavior of the functional groups was also observed. The frequency shifts of the carbonyl stretching at 1731 cm^{-1} in the DSDA I, II, III, and IV systems were lowered by 5, 5, 5, and 6 cm^{-1}, and those at 1780 cm^{-1} were shifted by 3, 3, 3, and 4 cm^{-1}, respectively. In addition, those of the N–H stretching band were shifted by 41, 40, 40, and 39 cm^{-1}, respectively. All the spectral behaviors of the carbonyl observed from 1731 and 1780 cm^{-1} and the N–H band at 3418 cm^{-1} are displayed in Figures 6–8, respectively, with open symbols. As shown in these figures, the frequency shifts of the DSDA systems are relatively smaller than those of the BTDAs, and the overall values measured from the eight systems are listed in Table 1.

We are not interested in individual values of the frequency shifts or the calculated areas from the T_g measurement or the k values for each blend system. The point we would like to emphasize is a trend of those values in the blends between BTDA and DSDA systems since the polyimides were synthesized using two different dianhydrides with the same four diamines. As shown in Table 1, the area or the frequency shift data imply that the BTDA-based systems have higher values than those in DSDA systems. Thus, this would indicate that the strength of the hydrogen bonding in PBI/BTDA systems is stronger than that in PBI/DSDA systems. We believe that the above results arose from the difference in the electron affinity in the two dianhydrides. Since DSDA has a higher electron affinity than BTDA,[27] it will make more stable polyimides with diamines; thereby the sulfone group in DSDA will generate more steric hindrance followed by a longer distance for the N–H group. Thus the longer distance between the functional groups is, the weaker the hydrogen bonding interaction that will be generated is.

Conclusion

The strength of the intermolecular interaction of hydrogen bonding for the miscible PBI/PI blends systems cured from PBI/PAAs has been studied by using DSC, DMTA, and FT-IR. Miscibility was suggested by the observation of an optically clear film and single composition dependent T_gs. The T_g diagram of the PBI/BTDA blend systems shows a larger deviation from the calculated values by the Fox equation than that in PBI/DSDA systems, indicating that the intermolecular interaction in the former systems is stronger than that in the latter ones. From the k values calculated by using Gordon–Taylor equation, the calculated areas of the BTDA systems are larger as well.

For the BTDA- and DSDA-based blend systems, the BTDA systems showed a larger extent of the band shifts of the functional groups than did the DSDA system for the carbonyl stretching near 1724/1731 and 1780 cm^{-1}

and the N–H stretching near 3418 cm^{-1}. Significant frequency shifts of the benzophenone carbonyl in BTDA and sulfone band in DSDA were not observed for the entire blends composition, implying that hydrogen bonding between the N–H and the carbonyl stretching of the five-membered imide ring is solely attributed to miscibility. Due to consistent results for the integrated area by the T_g diagram or the k values, and the degree of the frequency shifts of the functional groups, the strength of hydrogen bonding in the PBI/BTDA-based systems is stronger than that in the PBI/DSDA systems. This will be arise from the difference in electron affinity existing in the two dianhydrides; thus the longer the hydrogen-bonding distance is, the weaker hydrogen-bonding energy will be. The hydrogen-bonding distance and bonding energy between the functional carbonyl and the N–H groups are under calculation using the Monte Carlo method, and this work will be disclosed shortly.

References and Notes

(1) King, F. A.; King, J. J. *Engineering Thermoplastics*; Marcel Dekker Inc.: New York, 1985; p 315.
(2) Mittal, K. L. Ed., *Polyimides*, Plenum Press: New York, 1984; Vols 1 and 2.
(3) Bessonov, M. I.; Koton, M. M.; Kudryavtsev, V. V.; Laius, L. A. *Polyimides-Thermally Stable Polymers*; Plenum: New York, 1987.
(4) Sroog, C. E. *Macromol. Rev.* **1976**, *11*, 161.
(5) Adrova, N. A.; Bessonov, M. I.; Laius, L. A.; Rudakov, A. P. *Polyimides-A New Class of thermally stable Polymers*; Technomics: Lancaster, PA, 1970.
(6) Critchley, J. P.; Knight, G. J.; Wright, W. W. *Heat Resistance Polymers*; Plenum: New York, 1983.
(7) Cassidy, P. E. *Thermally Stable Polymers*; Marcel Dekker: New York, 1980.
(8) Levine, H. H. Polybenzimidazole. In *Encyclopedia of Polymer Science and Technology*; Mark, F. H., Norman, G. G., Norbert, M. B., Eds.; Wiley Interscience: New York, 1969; Vol. 11, pp 188–232.
(9) Leung, L.; Williams, D. W.; Karasz, F. E.; MacKnight, W. J. *Polym. Bull.* **1986**, *16*, 457.
(10) Guerra, G.; Choe, S.; Williams, D. J.; Karasz, F. E.; MacKnight, W. J. *Macromolecules* **1988**, *21*, 231.
(11) Stankovic, S.; Guerra, G.; Williams, D. J.; Karasz, F. E.; MacKnight, W. J. *Polym. Commun.* **1988**, *29*, 14.
(12) Guerra, G.; Williams, D. J.; Karasz, F. E.; MacKnight, W. J. *J. Polym. Sci., Polym. Phys. Ed.* **1988**, *26*, 301.
(13) Choe, S.; Karasz, F. E.; MacKnight, W. J. In *Contemporary Topics in Polymer Science, Multiphase Macromolecular Systems*; Cullbertson, B. M., Ed.; Plenum Press: New York, 1989; Vol. 6, 495.
(14) Choe, S.; MacKnight, W. J.; Karasz, F. E. *Polyimides; Material, Chemistry and Characterization*; Feger, C., Ed.; Elsevier Sci. Publishers B. V.: Amsterdam, 1989; Vol. 6, p 25.
(15) Choe, S.; Ahn, T. K. *Polymer (Korea)* **1990**, *14*, 115.
(16) Choe, S.; Ahn, T. K. *Polymer (Korea)* **1995**, *19*, 633.
(17) Kim, S. K.; Jeong, J. H.; Kim, H. S.; Choe, S. *Polymer (Korea)* **1992**, *16*, 249; Jeong, J. H.; Hwang, J. M.; Choi, H. J.; Choe, S. *Polymer (Korea)* **1994**, *18*, 677.
(18) Choe, S.; Ahn, T. K. *Polymer (Korea)* **1991**, *15*, 57.
(19) Gordon, M.; Taylor, J. S. *J. Appl. Chem.* **1952**, *2*, 495.
(20) Belorgey, G.; Prud'homme, R. E., *J. Polym. Sci., Polym. Phys. Ed.* **1982**, *20*, 191.
(21) Ting, S. P.; Pearce, E. M.; Kwei, T. K. *J. Polym. Sci., Polym. Lett. Ed.* **1980**, *18*, 201.
(22) Kwei, T. K. *J. Polym. Sci., Polym. Lett. Ed.* **1984**, *22*, 307.
(23) Rodrigne-Parada, J. M.; Percec, V. *Macromolecules*, **1986**, *19*, 55.
(24) Pugh, C.; Percec, V. *Macromolecules* **1986**, *19*, 65.
(25) Parmer, J. F.; Dickinson, L. C.; Chien, J. C. W.; Porter, R. S. *Macromolecules* **1989**, *22*, 1078.
(26) Masson, J. F.; Manley, R. S. J., *Macromolecules*, **1991**, *24*, 591.
(27) St. Clair, T. L. *Polyimides*; Wilson, D., Stenzenberger, H. D., Hergenrother, P. M., Eds.; Chapman and Hall: New York, 1990; Chapter 3.

MA951757R